

Origin and correlation of tuffs in the Permian Newcastle and Wollombi Coal Measures, NSW, Australia, using chemical fingerprinting

W. Kramer, G. Weatherall¹, R. Offler^{*}

Discipline of Geology, School of Geosciences, University of Newcastle, Callaghan, NSW 2308, Australia

Received 14 September 2000; accepted 18 June 2001

Abstract

Felsic tuffs are common throughout the Late Permian Newcastle and Wollombi Coal Measures (NCM, WCM) of the northern Sydney Basin. Petrographic studies reveal that they are composed of fragmented crystals of plagioclase, quartz, and less common degraded biotite and K-feldspar, together with lithic fragments and relict, altered glass shards. Alteration during burial at $T < 100$ °C has resulted in the formation of illite/smectite (I/S; I_{62-78}), kaolinite, siderite/ankerite and, in extreme circumstances, tonsteins dominated by I/S. The latter is formed by the alteration of vitric tuffs. Zr/TiO₂ and Nb/Y ratios, and rock-primordial and chondrite-normalised REE patterns ($La/Yb = 4.05$ to 11.37) indicate that the tuffs have been derived from rhyodacitic to dacitic, continental arc, calc-alkaline magmas.

The accuracy of a recent lithostratigraphic correlations between the NCM and the WCM has been tested by determining the chemical composition of four stratigraphically well defined tuffs in the NCM and comparing them with those obtained from tuffs of the WCM which are thought to be stratigraphically equivalent. The comparison was carried out using multivariate statistical analysis. The analysis revealed that two of the tuffs (Awaba, Nobbys) in the NCM could be distinguished; the others (Mt. Hutton, Warners Bay) showed considerable scatter. This contrasted with the tonsteins formed from the tuffs, which, apart from the Mt. Hutton Tuff, were able to be separated. In the WCM, three of the tuffs (Nalleen, unnamed tuff equivalent to the Mt. Hutton Tuff, Monkey Place Creek) could be separated; however, the fourth (unnamed tuff equivalent to the Warners Bay Tuff) exhibited some scatter. Treating tuffs in the WCM separately, as unknowns in the discriminant model to determine possible correlatives in the NCM, revealed that the Nalleen Tuff is equivalent to the Awaba Tuff in the NCM, confirming the lithostratigraphic correlation. The remainder of the tuffs in the WCM, however, show moderate to poor correlation with the proposed stratigraphically equivalents in the NCM. Thus, the analysis shows that correlation based on lithostratigraphic grounds may be incorrect. © 2001 Elsevier Science B.V. All rights reserved.

Keywords: Tuff; Geochemical fingerprint; Discriminant analysis

^{*} Corresponding author.

E-mail addresses: gweatherall@yahoo.com.au (G. Weatherall), robin.offler@newcastle.edu.au (R. Offler).

¹ Present address: Mining and Exploration Geological Services, P.O. Box 840, Toronto, NSW 2283, Australia.

1. Introduction

Tuffs are common throughout the Late Permian sequences of the Sydney Basin. They are the products of extensive volcanic activity, which distributed large amounts of ash over the Newcastle and Hunter Coalfields. Also present are tuffites formed by the reworking of the original ash deposits. The tuffs occur as continuous bands extending 150 km from the Newcastle Coalfield to the Hunter Coalfield (Fig. 1). Further, they vary in thickness from < 1 to 27 m, and generally thin towards the Hunter Coalfield. Previous studies in some locations of the Newcastle Coalfield have shown that each tuff represents several cycles of eruptive activity and deposition by a combination of pyroclastic fall, flow, and surge (Diessel, 1985; Gulson et al., 1990). However, the

morphology and composition of the tuffs examined in this study suggest that they were deposited as a series of ash falls. Many of the tuffs have been altered to tonsteins, which have been the subject of an earlier study by Loughnan (1962).

The Newcastle Coal Measures (NCM) of the Newcastle Coalfield and Wollombi Coal Measures (WCM) of the Hunter Coalfield currently have separate nomenclature for what is probably the same stratigraphy (Table 1; Stevenson, 1999). Attempts have been made to correlate lithostratigraphically the tuffs, coal seams and associated sediments of the NCM with those in the WCM. (Stevenson, 1999). However, in all lithostratigraphic correlations, there is always a degree of subjectivity and uncertainty. This uncertainty presents a problem in the exploration, evaluation, and current understanding of the

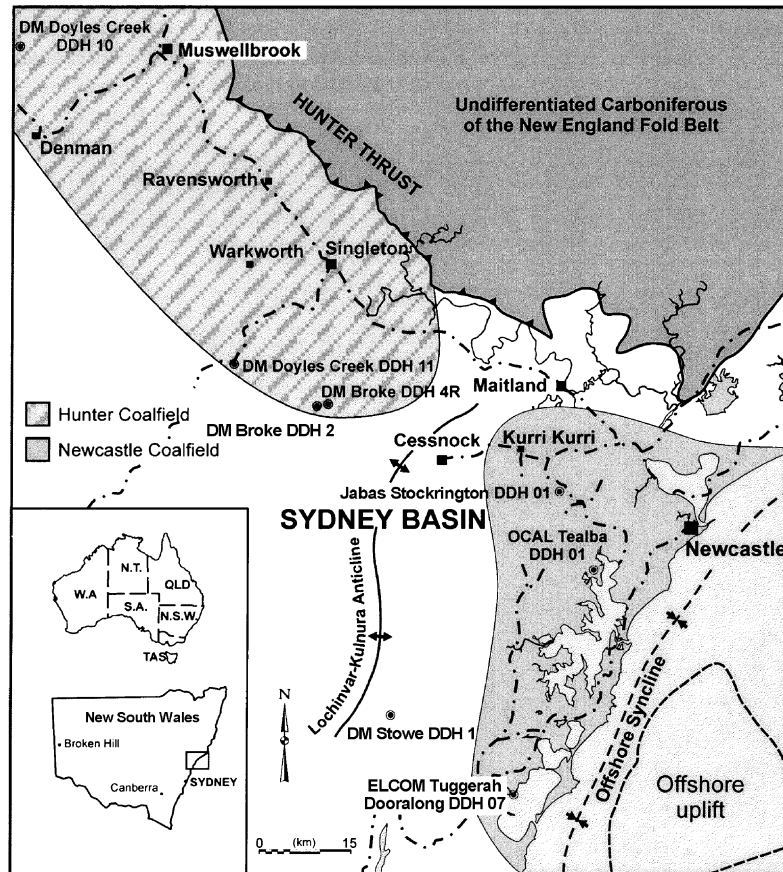


Fig. 1. Location of Newcastle and Hunter Coalfields, Offshore Uplift and drill holes from which samples were obtained.

Table 1

Lithostratigraphic correlation of Wollombi and Newcastle Coal Measures

WOLLOMBI COAL MEASURES	Glenn	Greigs Creek Coal			Vales Point seam	Moon Island Beach Formation		
		Redmanvale Creek Formation						
	Gallic	Dights Creek Coal	Hillsdale Coal Member		Wallarah seam			
					Great Northern seam			
	Subgroup		Nalleen Tuff Member			Awaba Tuff		
			Hobden Gully Coal M.			Fassifern seam Upper Pilot seam	Boolaroo Formation	
	Doyles Creek Subgroup	Waterfall Gully Formation			Mount Hutton Tuff Lower Pilot seam			
	Horshoe	Pinegrove Formation	Hambledon Hill Sand M.					
			Wyllies Flat Coal M.					
			Glengowan Shale M.					
			Eyriebower Coal M.					
			Longford Creek Silt. M.					
	Creek	Lucernia Coal	Rombo Coal Member					
			Hillside Claystone Member					
	Subgroup	Carramere Coal M.						
		Strathmore Formation				Hartley Hill Seam		
			unnamed Tuff			Warners Bay Tuff		
		Alcheringa Coal				Australasian seam		
			unnamed Tuff			Strockrington Tuff		
	Apple Tree Flat Subgroup	Charlton Formation			Montrose seam	Adamstown		
					Wave Hill seam	Formation		
			Clifford Formation	unnamed Tuff			Edgeworth Tuff	
Abbey Green Coal		Stafford Coal M.		Fern Valley seam	Nobbys Tuff			
				Victoria Tunnel seam				
	Monkey Place Creek Tuff M.							
			Nobbys seam	Lambton Formation				
			Dudley seam					
			Yard seam					
			Borehole seam					

NEWCASTLE COAL MEASURES	Glenn	Greigs Creek Coal			Vales Point seam	Moon Island Beach Formation		
		Redmanvale Creek Formation						
	Gallic	Dights Creek Coal	Hillsdale Coal Member		Wallarah seam			
					Great Northern seam			
	Subgroup		Nalleen Tuff Member			Awaba Tuff		
			Hobden Gully Coal M.			Fassifern seam Upper Pilot seam	Boolaroo Formation	
	Doyles Creek Subgroup	Waterfall Gully Formation			Mount Hutton Tuff Lower Pilot seam			
	Horshoe	Pinegrove Formation	Hambledon Hill Sand M.					
			Wyllies Flat Coal M.					
			Glengowan Shale M.					
			Eyriebower Coal M.					
			Longford Creek Silt. M.					
	Creek	Lucernia Coal	Rombo Coal Member					
			Hillside Claystone Member					
	Subgroup	Carramere Coal M.						
		Strathmore Formation				Hartley Hill Seam		
			unnamed Tuff			Warners Bay Tuff		
		Alcheringa Coal				Australasian seam		
			unnamed Tuff			Strockrington Tuff		
	Apple Tree Flat Subgroup	Charlton Formation			Montrose seam	Adamstown		
					Wave Hill seam	Formation		
			Clifford Formation	unnamed Tuff			Edgeworth Tuff	
Abbey Green Coal		Stafford Coal M.		Fern Valley seam	Nobbys Tuff			
				Victoria Tunnel seam				
	Monkey Place Creek Tuff M.							
			Nobbys seam	Lambton Formation				
			Dudley seam					
			Yard seam					
			Borehole seam					

stratigraphy of the WCM. Confident correlation between the NCM and WCM will allow more accurate assessment of the coal resources in the Hunter Coal-field by enabling correlation with known economic seams in the NCM.

The current study addresses this issue by using a chemostratigraphic approach which involves the determination of the chemical composition of stratigraphically well defined tuffs in the NCM. They are compared with the composition of tuffs in the WCM

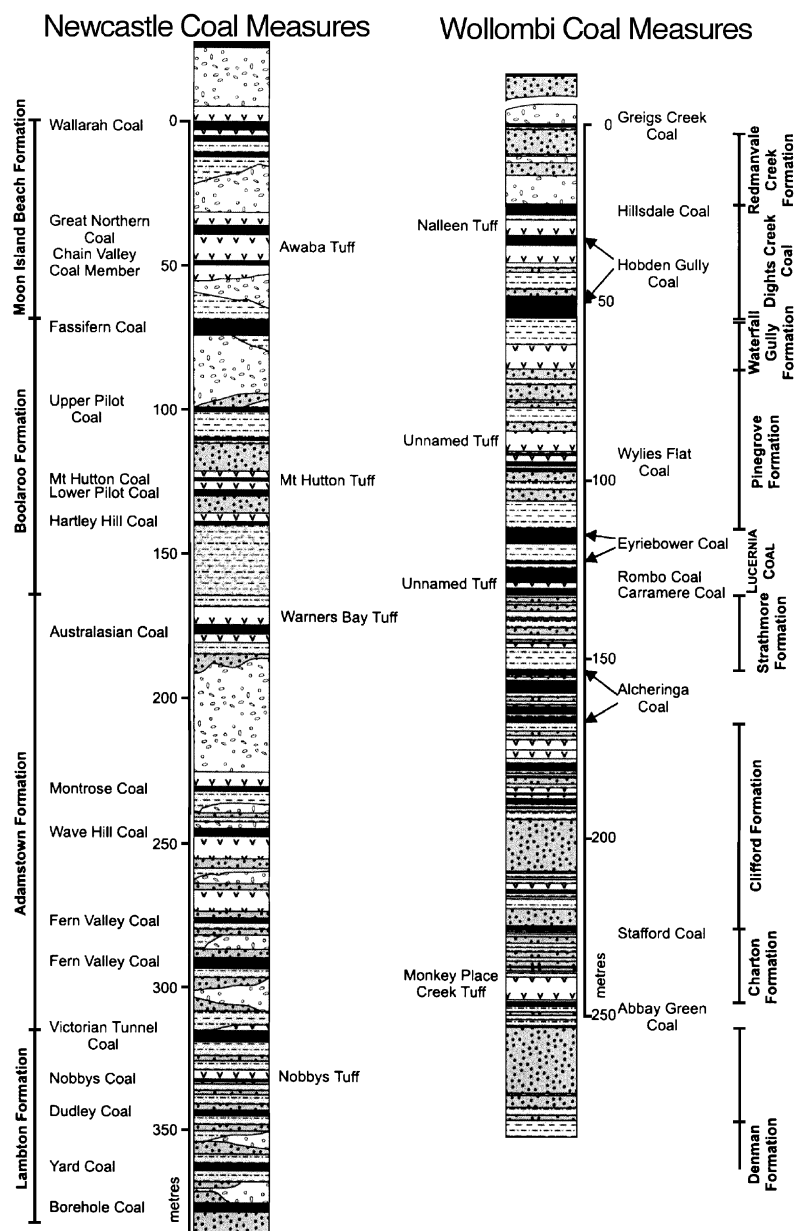


Fig. 2. Stratigraphic subdivision of the NCM (Crapp and Nolan, 1975) and WCM (Britten, 1972) showing the location of the tuffs analysed in this study.

Table 2
Representative analyses of tuffs in the Newcastle Coal Measures

Core	1	1	1	2	2	2	3	3	3	4	4	4
Tuff	1	2	3	1	2	4	1	3	4	1	2	4
Sample	AT8	MH5	WB2	AT3	MH4	NT7	AT3	WB5	NT4	AT8	MH3	NT3
SiO ₂	66.46	67.7	48.29	75.26	69.19	74.51	68.84	70.27	74.19	69.97	74.57	69.17
Al ₂ O ₃	14.33	12.65	22.63	12.56	15.73	9.8	15.43	13.74	14.6	15.37	13.88	17.79
Fe ₂ O ₃ T	4.63	2.1	2.33	1.02	1.93	0.74	1.7	3.01	1.12	2.7	1.93	1.71
MnO	0.03	0.03	0.02	0.01	0.00	0.02	0.02	0.03	0.00	0.04	0.00	0.01
MgO	1.63	1.53	1.64	1.1	1.28	0.58	0.92	0.73	1.14	1.14	1.03	1.25
CaO	0.74	3.99	7	0.84	0.29	3.87	3.16	1.85	0.84	0.94	0.42	0.86
Na ₂ O	1.02	1.28	1.11	1.89	1.11	1.8	3.46	3.18	1.04	1.26	1.33	1.44
K ₂ O	2.67	1.5	5.58	0.3	3.69	2.13	1.33	0.21	2.56	3	1.92	2.81
TiO ₂	0.36	0.33	0.19	0.25	0.23	0.15	0.49	0.14	0.22	0.31	0.21	0.3
P ₂ O ₅	0.02	0.08	0.03	0.02	0.06	0.05	0.18	0.02	0.07	0.02	0.05	0.08
LOD	3.01	2.28	1.73	2.42	2.81	1.04	1.05	0.72	0.66	0.87	1.04	0.86
LOF	4.96	7.03	9.63	4.3	3.55	5.47	3.58	6.18	3.64	4.46	3.56	3.71
Total	99.86	100.50	100.17	99.99	99.87	100.14	100.15	100.8	100.9	100.06	99.95	99.98
<i>Trace elements (ppm)</i>												
Ba	593	908	563	647	520	563	656	712	567	788	888	465
Zn	94	42	88	57	55	38	50	49	26	28	11	95
S	132	127	127	76	151	113	230	285	152	161	117	114
Sr	191	462	127	219	83	190	500	345	226	304	225	168
V	16	5	< 3	< 3	21	< 3	23	8	10	< 3	5	12
Ga	20	15	28	13	19	11	39	40	43	39	34	48
Zr	264	181	223	126	159	94	209	147	147	228	117	198
Cs	< 20	< 20	< 20	< 20	40	< 20	< 20	36	< 20	< 20	< 20	< 20
Pb	32	22	43	33	33	24	16	26	33	31	35	48
Rb	106	66	270	23	153	82	68	21	98	168	91	101
Cr	< 5	< 5	< 5	< 5	< 5	< 5	< 5	< 5	< 5	< 5	< 5	< 5
Y	5	22	43	7	11	17	15	18	20	13	13	13
As	< 3	< 3	< 3	< 3	< 3	< 3	8	5	< 3	3	< 3	< 3
Co	21	12	< 10	11	< 10	12	29	10	11	< 10	< 10	11
Cu	< 3	< 3	< 3	< 3	< 3	< 3	< 3	< 3	< 3	< 3	< 3	< 3
Cl	< 20	< 20	< 20	< 20	178	< 20	30	< 20	< 20	62	24	< 20
Hf	8.53	7	9	4.73	6.03	3.6	23	18	17	21	15	20
Nb	< 5	< 5	6	< 5	< 5	< 5	< 5	< 5	< 5	< 5	< 5	< 5
Ni	< 3	5	< 3	< 3	4	< 3	< 3	< 3	< 3	< 3	< 3	< 3
Th	27.70	20	24	27.90	27.40	19.3	17	13	29	31	22	34
U	13	< 5	< 5	< 5	< 5	< 5	< 5	< 5	< 5	< 5	5	< 5
Sn	< 10	< 10	< 10	< 10	< 10	< 10	< 10	< 10	< 10	< 10	< 10	< 10
Ta	1.00			0.95	1.06	0.76						
La	26.34	50	57	28.5	34.2	24.63	26	23	39	11	14	12
Ce	53.2	51	68	58.84	74.73	53.02	56	62	62	35	65	77
Nd	19.07			18.71	32.12	23.13						
Sm	3.23			2.88	6.45	4.35						
Eu	0.52			0.38	0.71	0.42						
Tr	0.42			0.35	0.7	0.66						
Ho	0.61			0.56	0.89	1.18						
Yb	1.62			1.82	2.01	4.07						
Lu	0.26			0.28	0.3	0.63						
Rb/Sr	0.55	0.14	2.13	0.11	1.84	0.43	0.14	0.06	0.43	0.55	0.40	0.60

Core: 1 = Elecom Tuggerah Dooralong; 2 = DM Stowe DDH1; 3 = JABAS Stockrington DDH1; 4 = OCAL Teralba DDH7.

Tuff: 1 = Awaba; 2 = Mount Hutton; 3 = Warners Bay; 4 = Nobbys Tuff.

REE, Hf, Ta and Th for AT8, AT3, MH4 and MH4 by NAA; the remaining samples by XRF.

Table 3
Representative analyses of tuffs in the Wollombi Coal Measures

Core	1	1	1	2	2	2	2	3	3	3	4	4
Tuff	1	2	4	1	2	3	4	2	3	4	2	4
Sample	NT5	MH5	MPC2	NT5	MH5	WB2	MPC2	WB1	MH2	MPC3	WB1	MPC3
SiO ₂	72.12	79.85	77.95	68.57	76.6	81.05	70.14	78.66	79.6	78.67	76.82	73.83
Al ₂ O ₃	18.72	13.32	14.67	22.73	14.07	14.04	21.86	14.4	13.99	13.85	17.43	15.06
Fe ₂ O ₃	2.29	1.61	1.39	2.42	2.45	0.74	0.9	2.12	1.58	1.71	0.97	1.89
MnO	0.01	0.01	0	0.01	0.02	0.01	0	0.01	0	0	0.01	0.01
MgO	3.02	0.88	0.83	1.66	1.07	0.48	0.67	1.78	1.62	1.94	0.89	0.84
CaO	1.7	0.63	1.09	1.23	1.37	0.53	0.88	0.4	0.55	0.68	0.7	2.72
Na ₂ O	1.11	1.08	1.85	1.74	1.67	2.57	2.03	1.55	1.28	1.99	2.37	2.92
K ₂ O	0.5	2.32	1.9	1.17	2.41	0.41	3.09	0.83	1.11	0.88	0.56	2.16
TiO ₂	0.5	0.22	0.25	0.47	0.25	0.17	0.34	0.21	0.23	0.22	0.2	0.46
P ₂ O ₅	0.02	0.07	0.07	0.02	0.08	0.02	0.1	0.04	0.04	0.06	0.06	0.1
LOD	6.95	2.325	2.44	6.69	2.04	3.18	2.11	0.99	0.85	0.75	0.77	0.39
LOF	5.55	3.055	3.16	6.01	3.65	2.82	3.88	3.78	4.31	3.79	6.2	6
Total	100.09	100.04	99.87	100.29	100.37	100.13	100.23	100.13	100.02	100.55	100.65	100.25
<i>Trace elements (ppm)</i>												
Ba	188	601	492	572	640	637	598	427	639	504	462	885
Zn	59	40	54	101	44	44	56	101	17	22	107	30
S	99	72	80	104	106	318	87	76	97	137	125	167
Sr	457	304	230	601	284	244	251	272	427	293	256	435
V	30	15	7	26	20	6	18	4	3	12	3	24
Ce	54	46	63	53	44	37	65	44	48	58	66	57
Ga	20	17	20	24	17	18	28	41	41	42	45	43
Zr	189	167	186	190	188	163	250	118	115	129	171	247
Cs	20	22	20	20	20	20	25	20	20	20	20	20
Pb	43	32	35	48	32	21	46	24	28	36	33	21
Rb	28	88	64	68	100	23	101	50	62	40	29	73
Cr	5	5	5	5	15	5	5	5	5	5	5	5
La	30	26.37	38.2	39.94	28	27.6	46	31	15	32	46	16
Y	12	22	19	24	27	21	30	6	14	33	14	17
As	3	3	3	3	3	5	3	3	3	3	3	3
Co	10	10	10	15	10	11	11	10	10	10	10	14
Cu	3	3	3	3	3	3	3	3	3	3	3	3
Cl	23	27	20	32	20	20	20	20	20	20	20	20
Hf	8	5.8	6.75	7.3	7	5.22	9	14	16	17	18	26
Nb	7	7	5	5	10	6	5	5	5	5	5	5
Ni	3	3	3	3	3	3	3	3	3	3	3	3
Th	35	20.5	24.5	41.1	25	15.2	41	13	24	28	23	19
U	7	5	5	9	13	5	22	5	5	5	6	5
Sn	10	10	10	10	10	10	10	10	10	10	10	10
Nd		25.48	36.77	26.48		25.98						
Sm		4.91	6.87	4.19		5.02						
Eu		0.69	0.72	0.73		0.56						
Tr		0.67	0.83	0.62		0.64						
Ho		1.03	1.18	1.01		0.85						
Yb		2.66	3.23	3.11		1.95						
Lu		0.4	0.5	0.48		0.29						
Rb/Sr	0.15	0.53	0.34	0.36	0.53	0.14	0.4	0.42	0.54	0.31	0.17	0.29

Core: 1 = DMBroke D2; 2 = DMBroke 4R; 3 = DMDoyles Creek 10; 4 = DM Doyles Creek 11.

Tuff: 1 = Nalleen Tuff; 2 = "Warners Bay Tuff"; 3 = "Mt. Hutton Tuff"; 4 = Monkey Place Creek Tuff.

REE, Hf, Ta and Th for MH5, MPC2, NT5 and WB2 by NAA; the remaining by XRF.

using multivariate statistical analysis. It will be shown that most tuffs and their altered equivalents (tonsteins) have unique chemical signatures, which allows correlation within individual coal measures. However, limited success has been attained in correlating the tuffs between the coal measures, showing that the lithostratigraphic correlation proposed by Stevenson (1999) may be incorrect. The study also involved the determination of the composition of the magmas from which the tuffs were derived and the setting in which they were erupted. These aspects have not been addressed in previous studies of the tuffs.

1.1. Depositional environment of the tuffs

The Sydney Basin evolved from a rift basin to a foreland basin in the late Early Permian (Hawley and Brunton, 1995). At that time, volcanism associated with a continental arc (see later discussion) east of the present coastline resulted in ash falls interrupting the normal sedimentation patterns. The ash and sediments accumulated in a southwest-prograding siliciclastic wedge within a north–south trending half-graben between the Lochinvar Anticline and an “upthrust” Offshore Uplift (Fig. 1; Herbert, 1994). Deposition occurred during a prolonged marine regression, a result of uplift of the southern New England Orogen (SNEO) during the Hunter–Bowen Orogeny (Collins, 1994). Variations in relative sea level controlled nonvolcanic and volcanoclastic sedimentation in brackish lakes and lagoons landward of the marine barrier shoreline (Herbert, 1994, 1997; Hawley and Brunton, 1995). Uplift of the SNEO caused a relative sea-level fall, resulting in river systems eroding and transporting previously deposited sediments into the basin. A lack of erosion during sea level highstands resulted in westward progradation of deltas, due to the Offshore Uplift, dominating sediment supply (Herbert, 1994). Late Permian raised peats flourished when not inundated with volcanic ash (Herbert, 1997). The coal seams that subsequently formed thicken eastward as a result of faster subsidence of the Offshore Syncline (Herbert, 1997). The swamps in which the coal formed changed with time from brackish, wet forested swamps, to progressively fresh water, dry forested swamp (Herbert, 1997). Deposition of the coal mea-

sures ceased at the end of the Permian (251 Ma; Young and Laurie, 1996) when continued subsidence followed by rapid uplift of the SNEO, resulted in

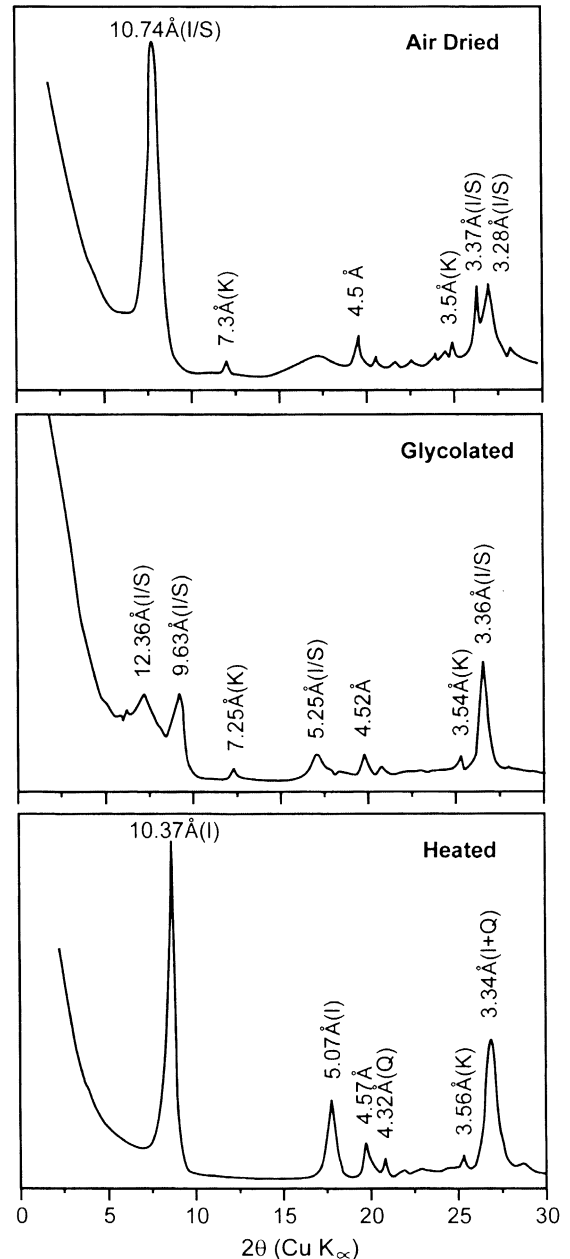


Fig. 3. XRD patterns obtained from the <2- μ m fraction of SMH5. The splitting of the 10.74 Å air-dried peak following glycolation indicates the presence of illite–smectite.

deposition of alluvial floodplain sediments of the Lower Narrabeen Group (Hawley and Brunton, 1995).

Deposition controlled by changes in relative sea levels are reflected in the stratigraphy observed in the cores examined in this study. Tuffs found in the NCM are interbedded with deltaic mudstone and shale sequences which fine upwards and which are often overlain by coal. It is no coincidence that the thickest tuffs are found within these strata, as a lower deltaic coal-forming environment is ideal for preserving the large quantity of ash falls characteristic of the Late Permian (Herbert, 1994). The WCM occur further northwest and landward of the palaeo-shoreline and, therefore, have a stratigraphy that reflects this. Thus, the tuffs of the WCM are commonly found intercalated with sandstone sequences,

which represent fluvial and upper deltaic depositional systems.

1.2. Correlating tuffs using geochemical fingerprinting

It has been known since the early 1920s that the geologically instantaneous nature of fallout tuffs allows them to be used as regional time surfaces. However, previous attempts by various authors to correlate tuff layers in sedimentary basins have been unsuccessful because of the large number of beds, their mineralogical similarity over large distances, and lack of persistent macroscopically and microscopically identifiable features (see discussion by Cullen-Lollis and Huff, 1986; Kolata et al., 1986; Huff and Kolata, 1989). Geochemical fingerprinting

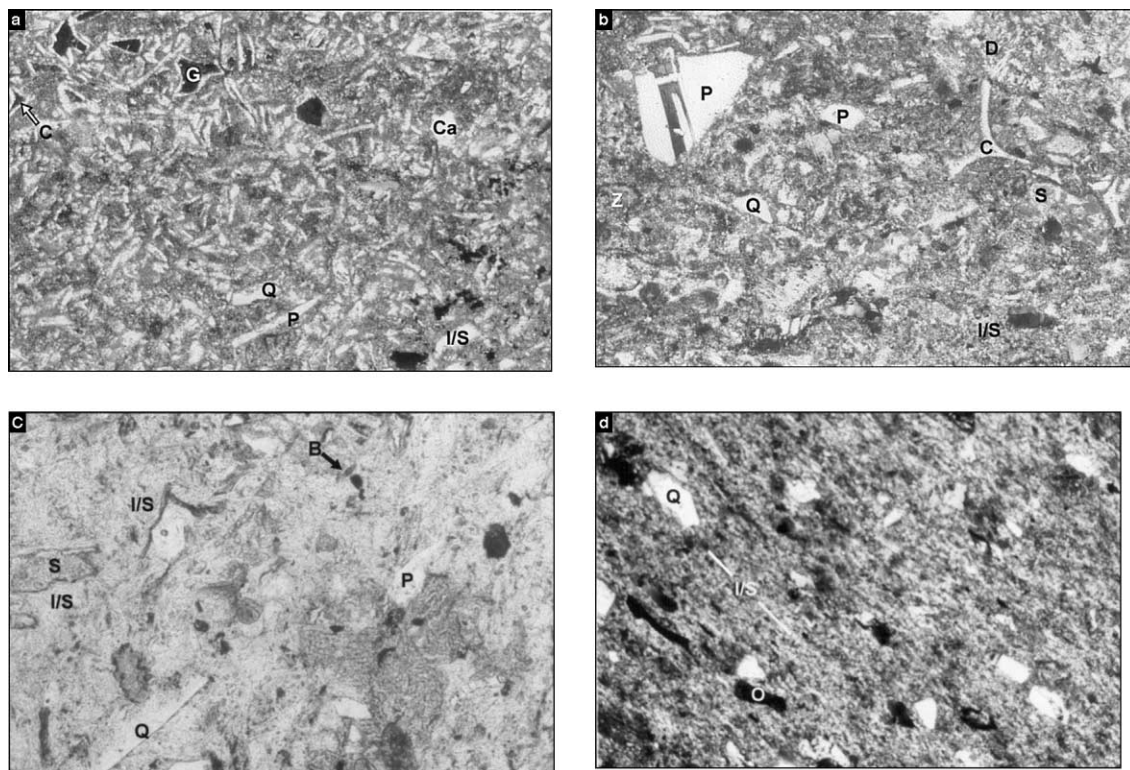


Fig. 4. (a) Vitric-crystal tuff showing vitriclastic texture. The shards are platy (P) and cusps (C) and are replaced by illite-smectite (I/S). Sample 16185/MDCK11. Cross polars. Length of field is 0.7 mm. (b) Crystal-vitric tuff exhibiting cusps (C) shards, plagioclase (P), zircon (Z) and a dacite clast (D). Siderite (S) and I/S in groundmass. Sample 16225B/DMB4R. Cross polars. Length of field is 1.4 mm. (c) Crystal tuff showing siderite aggregates (S), quartz (Q), plagioclase (P), degraded biotite (B). Groundmass consists of I/S. Sample 16315/ENT5. Plane polarised light. Length of field is 1.4 mm. (d) Tonstein containing quartz (Q), altered opaque minerals (O) surrounded by oriented I/S. Sample 16262/TWB2. Cross polars. Length of field is 2.8 mm.

as a possible tool for correlation has only been developed in the past 15 years (Huff and Kolata, 1989). When geochemical data are combined with multivariate discriminant analysis to identify a unique fingerprint for individual volcanic beds, a more precise method of chronostratigraphic correlation results (Mitchell et al., 1994).

Successful correlation based on geochemical fingerprinting of K-bentonite beds of the Decorah Subgroup, Mississippi Valley, has been detailed in many papers (Huff, 1983; Cullen-Lollis and Huff, 1986; Kolata et al., 1986, 1987; Huff and Kolata, 1989, 1990). The separate beds are distinguishable when chemical data are plotted on territorial maps defined by the two major discriminant functions. This regional correlation was carried out over 900 km and has resulted in an improved interpretation of Middle Ordovician palaeoenvironments and palaeogeography (Kolata et al., 1987). A much larger scale correlation was achieved using the same approach to correlate a single tuff horizon on two separate continents, the Millbrig K-bentonite in eastern North America with the “Big-Bentonite” in northeastern Europe (Huff et al., 1992). This correlation has facilitated the reconstruction of Ordovician plate boundaries.

In view of the successful application of geochemical fingerprinting of tuffs in other continents, this approach was considered worthy of using in the northern Sydney Basin, where tuffs are common in Late Permian coal measures and where problems of stratigraphic correlation have arisen between adjacent coalfields. This type of study is unique in that it deals with the chemical signature of tuffs and tonsteins rather than bentonites, which have been the focus of other studies (Huff et al., 1997 and references therein). Further, to our knowledge, this chemostratigraphic approach has not been applied to coal measures.

2. Methods

Samples of core containing the Nobbys, Warners Bay, Mount Hutton and Awaba Tuffs in the NCM and their possible stratigraphic equivalents in the WCM, were chosen for analysis (Fig. 2); 72 samples

were obtained from the WCM and 101 samples from the NCM. To avoid inaccurate results, selection of samples was based on those areas of the tuff least contaminated by clastics and organic matter and which were not reworked. As noted earlier, each tuff contains several units representing cycles of eruptive activity; therefore, our sampling strategy involved taking a sample from each cycle with the aim of obtaining a true representation of the entire tuff bed. Samples were acquired from eight widely spaced drill holes in the Newcastle and Hunter Coalfields (Fig. 1). Representative analyses are shown in Tables 2 and 3.

2.1. X-ray diffraction

Each sample was crushed for 20 s in a tungsten carbide Tema ring mill and the <2- μ m fraction separated from the powder and sedimented onto glass slides. Diffractograms were obtained from air-dried, glycolated and heated (550 °C) slides, and analysed using a Philips automated PW1732/10 X-ray diffractometer, CuK α radiation, graphite monochromator, and 40 kV/30 mA. Samples were scanned over the range $2\theta = 2\text{--}30$ at $0.02^\circ 2\theta/\text{s}$ using divergence and scatter slits of 1° and a receiving slit of 0.2 mm. Identification of clay mineralogy and determination of the percentage of illite in

Table 4
Representative analyses of altered biotites

Wt. %	WCM Mt. Hutton tuff		Rockisle N4 ^a
	1	2	3
SiO ₂	39.37	35.20	36.16
TiO ₂	4.07	3.63	3.99
Al ₂ O ₃	29.72	22.10	14.40
FeO	9.61	19.04	21.13
MnO	0	0.21	0.40
MgO	3.46	7.83	9.83
CaO	0	0	0.03
Na ₂ O	0	0	0
K ₂ O	0.91	2.91	9.60
Total	87.14	90.92	95.55

^aGranodiorite sample from Hillgrove Supersuite (Landenberger, 1996) was included for comparison.

illite–smectite was determined following the methods of Moore and Reynolds (1989; Fig. 3).

2.2. XRF / INAA

Less altered samples were crushed for 2 min and strongly altered samples for up to 5 min to obtain a

homogeneous powder suitable for analysis. XRF analyses were carried out on fused glass discs, using a Philip's PW1404 Wavelength Dispersive Sequential XRF, controlled by Philips X40 software. A low-dilution fusion technique was employed in the production of the discs (Eastell and Willis, 1990). Representative analyses of the tuffs and tonsteins are

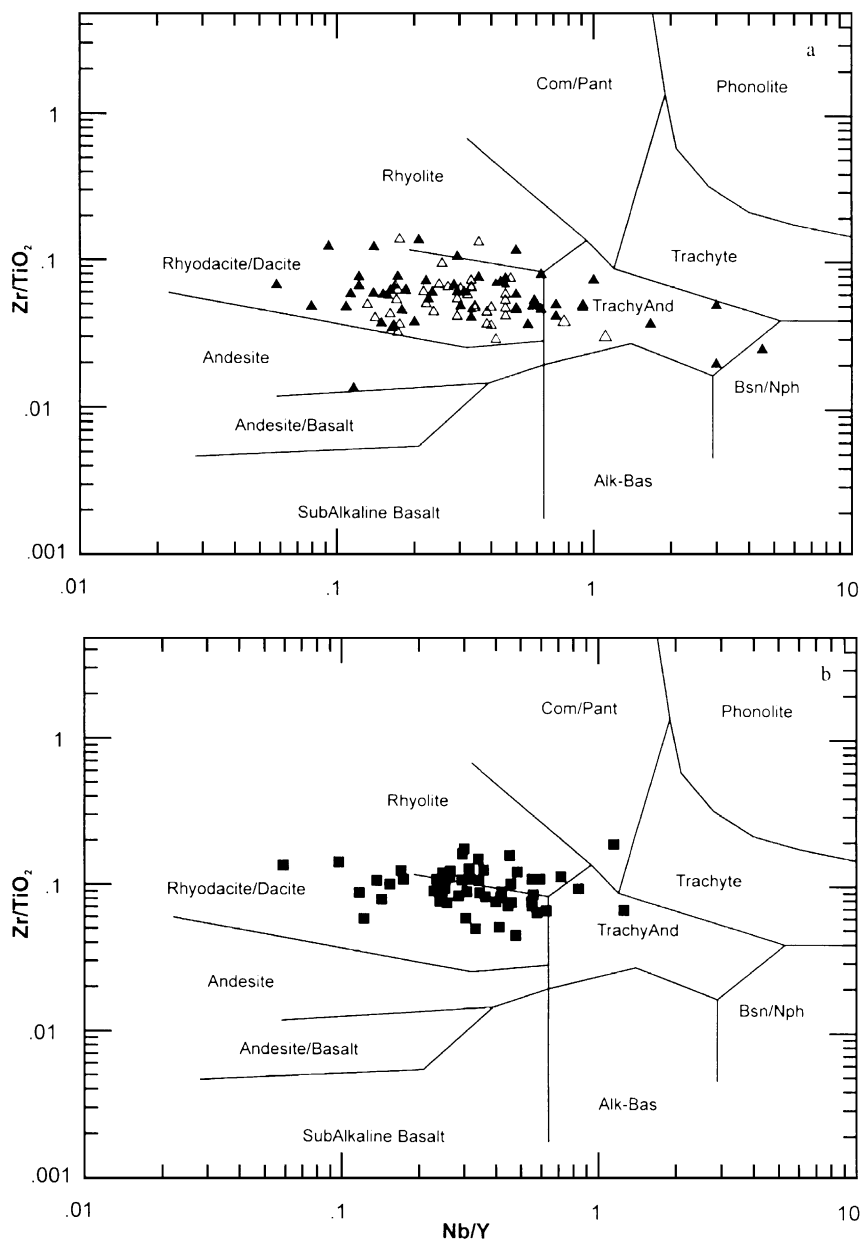


Fig. 5. TiO_2/Zr versus Nb/Y for tuffs (open Δ) and tonsteins (closed \blacktriangle). (a) NCM; (b) WCM.

shown in Tables 2 and 3. The REE contents of eight samples were determined by Instrumental Neutron Activation Analysis (INAA) at Becquerel Laboratories, Lucas Heights, Sydney.

2.3. SEM/EDS

The chemical composition of carbonates, feldspars, degraded biotite and illite–smectite (I/S) have been obtained from polished thin sections of the samples, using a JEOL JSM-840 scanning electron microscope, attached to which is an Oxford ISIS 200 EDS operating at 2.5 mA and 15 kV. Standards used include Na_2CO_3 , Albite, MgO , Al_2O_3 , Wollastonite, Orthoclase, Rutile, Cr, Mn, and haematite. Data reduction was carried out on an on-line computer using SEMQUANT.

3. Characteristics of tuffs

3.1. Mesoscopic features of tuffs

In the Newcastle and Hunter Coalfields, the tuffs are generally fine silt size (< 2 mm) and range in

colour from white to grey/brown, although most are grey/beige and some have a greenish tinge. Those in the NCM exhibit more syn-depositional structures than their counterparts in the WCM. They are commonly laminated and plant detritus is often concentrated at the base of units. In certain horizons, the latter is associated with flattened mud clasts. Laminations in some samples are convoluted, indicating that soft sediment deformation has taken place. Grading, both normal and reverse, is present in the tuffs and is better developed in the finer-grained versions. Soft sediment deformation and cross-stratification due to resedimentation is more common in the NCM. Cross-stratification is particularly common in the Awaba Tuff.

Different eruptive cycles are represented within single tuff horizons by a number of fining upwards units, each defined by unique depositional structures. Thus, in one cycle, cross-stratification may be common, in another, convolute bedding. Each unit represents a series of ash fall deposits possibly derived from different vents or volcano(es) in which magma is evolving.

Tuffs in both coal measures have undergone diagenetic alteration. Alteration is greatest in the NCM

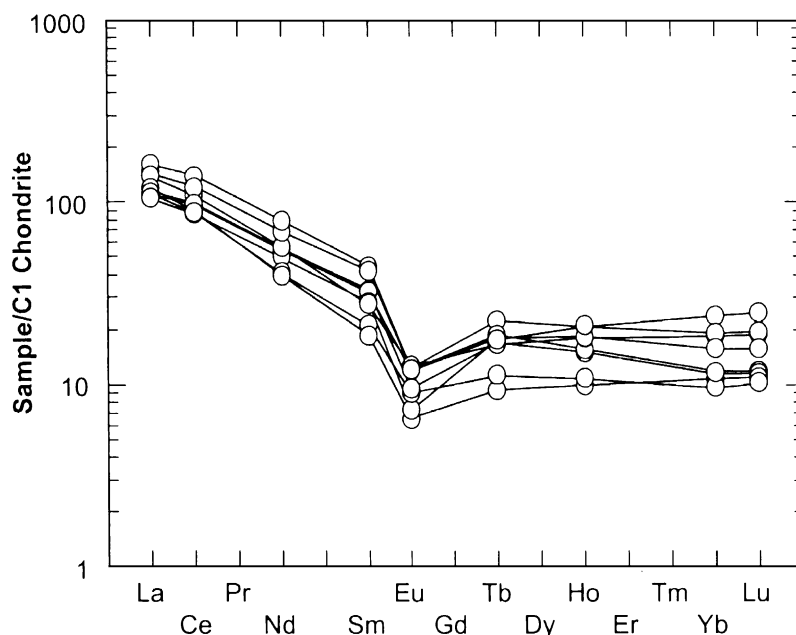


Fig. 6. Chondrite normalised patterns of tuffs in the NCM and WCM. Normalising values from Sun and McDonough (1989).

and leads to the formation of tonsteins when it is extreme. The distribution of tonsteins is not significantly affected by depth of burial, as tuffs throughout the NCM show the same degree of alteration. However, alteration differs somewhat within the tuffs with the base and top of each tuff exhibiting greater alteration. This can be attributed to a leaching effect whereby fluids from adjacent strata alter the composition of the tuff (Bohor and Triplehorn, 1993). Some tuffs are extensively veined by calcite and siderite, others contain ankerite in some horizons.

3.2. Petrography

Thin section examination reveals that the tuffs are matrix-supported and consist of vitric, crystal and lithic fragments, the proportions differing between samples within the same tuff horizon (Fig. 4a–c). However, a lithic component is only present in a few samples, particularly those from the NCM. The crystal component is defined by a variety of angular to semi-euhedral minerals, which vary in size and amount of fracturing, and which range from well sorted to poorly sorted. Bedding, where developed, is defined by an alignment of crystals, particularly biotite, or by organic detritus.

The crystal component of the tuffs consists mainly of quartz, plagioclase ($An_{54}Ab_{42}Or_4$ – $An_{33}Ab_{59}Or_8$) and biotite (Fig. 4a–c). Quartz grains are commonly embayed and can vary in diameter from < 0.02 to 0.5 mm and rarely show undulose extinction. Plagioclase is commonly lath-shaped, ranges in length from 0.1 to 0.3 mm and exhibits oscillatory zonation. Rare K-feldspar ($Or_{55}Ab_{34}An_{11}$ – $Or_{77}Ab_{21}An_2$) is present in some samples. Plagioclase can show alteration to clay at grain boundaries and along fractures and also to calcite. Ti-rich degraded biotite is present in most of the samples but differs in abundance and size (0.1 to > 1.2 mm). SEM/EDS analyses indicate that an increase in degradation is reflected by a loss in K and a gain in H_2O (Table 4). Opaque minerals are an uncommon phase in both coal measures, and appear to be slightly more common in the WCM. In the less-altered samples, magnetite is the opaque mineral present. Accessory minerals found in some tuffs include zircon and apatite. Siderite and calcite commonly replace plagioclase and siderite occurs as aggregates in the clay-rich matrix.

Lithic fragments are generally subrounded and rarely angular in the NCM, but are notably more angular in the WCM and average ~0.3 mm in diameter. Most lithic fragments appear to be the recrystallised groundmass of silicic volcanic rocks or dacite, the latter showing plagioclase phenocrysts set in a fine-grained groundmass (Fig. 4b).

The tuffs in both coal measures show varying degrees of alteration with clays and carbonates being dominant. Those samples which are rich in the vitric

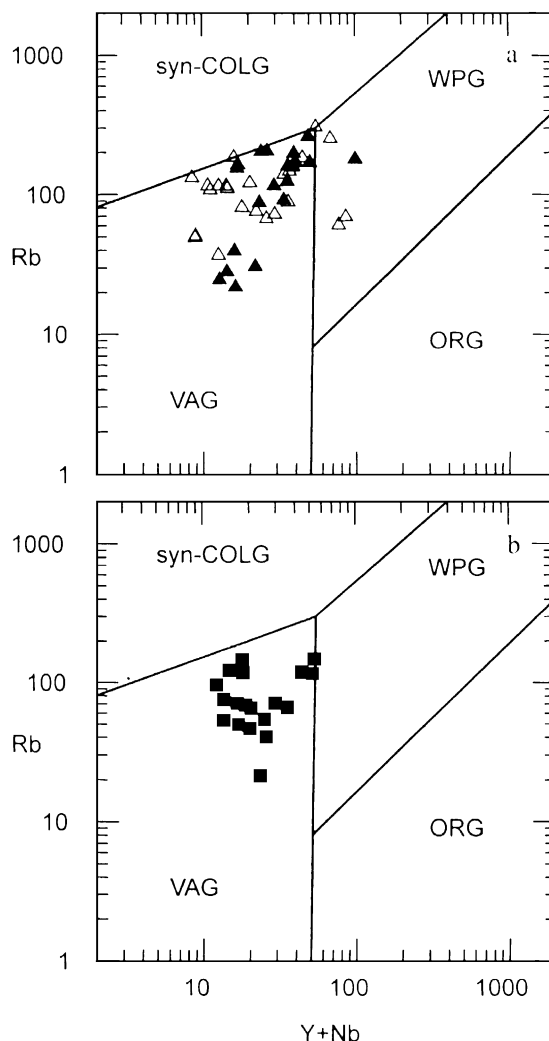


Fig. 7. Plot of Rb/Zr versus Y for tuffs of the NCM and WCM. VAG—volcanic arc granite; ORG—oceanic ridge granite; WPG—within-plate granite; syn-COLG—syn-collisional granite. Symbols as in Fig. 5.

component are commonly altered to claystones. In a few, a relict vitroclastic texture is evident (Fig. 4a), but in most, the angular outlines of the nonwelded shards have been obliterated. The clays in the claystones are oriented parallel to bedding and commonly define one or two “foliations” oblique to bedding (Fig. 4d). XRD reveals that the clays are I/S and kaolinite, the former containing 62–78% illite and which has both ordered and random interstratification (Kramer, 1999). The carbonates in the claystones and the less altered tuffs are ankerite, siderite, and less commonly calcite. According to the definition of Bohor and Triplehorn (1993), the claystones are smectitic tonsteins since their precursors have formed in a coal-forming environment. The composition of I/S indicates that the tonsteins have formed under early diagenetic zone conditions (Fig. 2.1 from Merriman and Peacor, 1999), over a temperature range of 60–90 °C (Hower et al., 1976).

3.3. Mode of deposition

Studies by Kramer (1999) suggested that the tuffs in the NCM were deposited by fall-out from a turbulent ash cloud carrying suspended ash. Morphological evidence supporting this interpretation is the

laterally continuous nature of the beds as well as fine grain size of particles, alignment of minerals, graded bedding, laminations, and planar lower contacts. In some tuffs, there is evidence for movement and resedimentation of ash occurring after deposition. Post-depositional movement of ash was likely to have been caused by seismic activity and is manifest as convolute bedding and cross-stratification. Disruption of sediments and the shifting of grains results in lateral aggradation of the ash to form the small-scale cross-stratification observed in the NCM tuffs.

3.4. Discrimination of magma series

As discussed previously, petrographic examination revealed that quartz, plagioclase, biotite and, less commonly, K-feldspar are present in the tuffs, and that dacite is a lithic component. Further, the plagioclase is moderately An-rich. These features suggest that the magmas prior to eruption had a rhyodacitic to dacitic composition. Evidence supporting this interpretation is seen when the data are plotted on a discrimination diagram of Winchester and Floyd (1977), which involves the immobile elements Ti, Zr, Nb, and Y to classify magma types (Fig. 5a,b). It shows that the majority of the samples

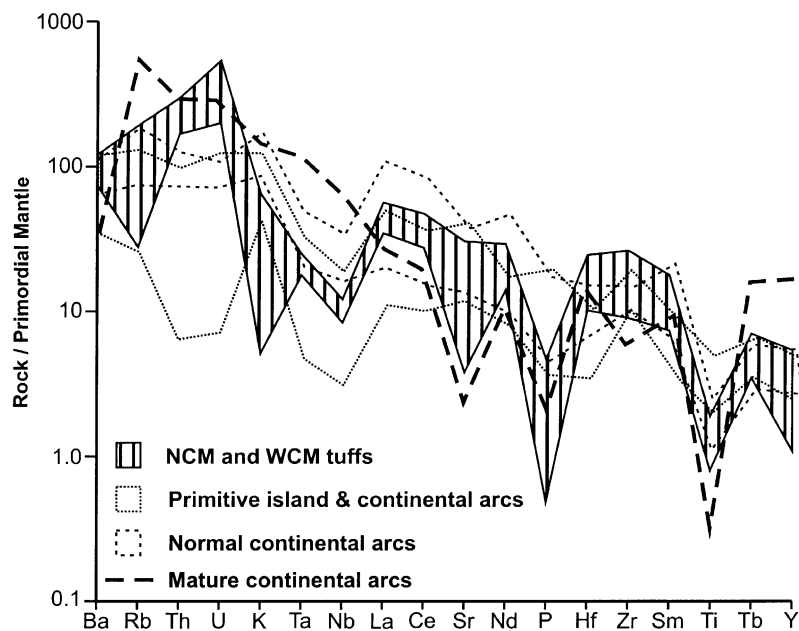


Fig. 8. Rock/primordial mantle plots for NCM and WCM. Normalising values from Sun and McDonough (1989).

plot in the rhyodacite/dacite field. LREE-enriched ($\text{La}/\text{Yb} = 4.05$ to 11.37) and flat-HREE chondrite-normalized patterns of the tuffs indicate that they were derived from calc-alkaline magmas (Fig. 6; Jakeš and Gill, 1970).

3.5. Tectonic setting

To determine the possible tectonic setting of the volcanoes responsible for the widespread ash fall deposits during the deposition of the Late Permian coal measures, analyses of the less-altered tuffs have been plotted on the Rb versus Y + Nb diagram of Pearce et al. (1984), which is used for the discrimination of the tectonic settings of granitic rocks (Fig.

7). The majority of the tuffs plot within the “volcanic-arc granite” field, suggesting derivation of the ash from an arc source. However, this diagram must be interpreted with caution as the compositions of the tuffs may reflect the source geochemistry rather than the tectonic setting (Rollinson, 1993).

If it is accepted that the tuffs have been derived from an arc source, were they derived from volcanoes in an island- or continental-arc setting? Their rock/primordial mantle patterns (Fig. 8), Nb, Y contents, and Rb/Zr ratios (Brown et al., 1984; Ewart and Chappell, 1989; Tables 2 and 3), suggest that a normal calc-alkaline, continental-arc setting existed in the Late Permian. Evidence supporting this interpretation is the LREE enrichment apparent in

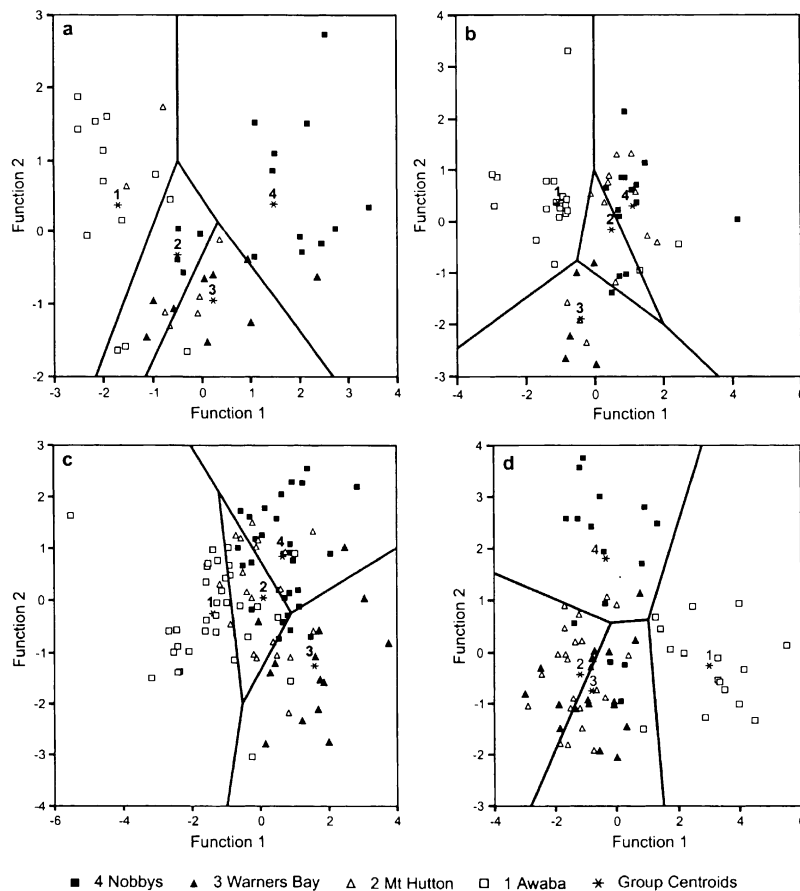


Fig. 9. Territorial maps: (a) tuffs—NCM; (b) tonsteins—NCM; (c) tuffs and tonsteins—NCM; (d) tuffs—WCM; (e) Nalleen Tuff; (f) unnamed tuff 2; (g) unnamed tuff 3; (h) Monkey Place Creek. (e), (f), (g), and (h) were treated as unknowns and compared against discriminant model in (c).

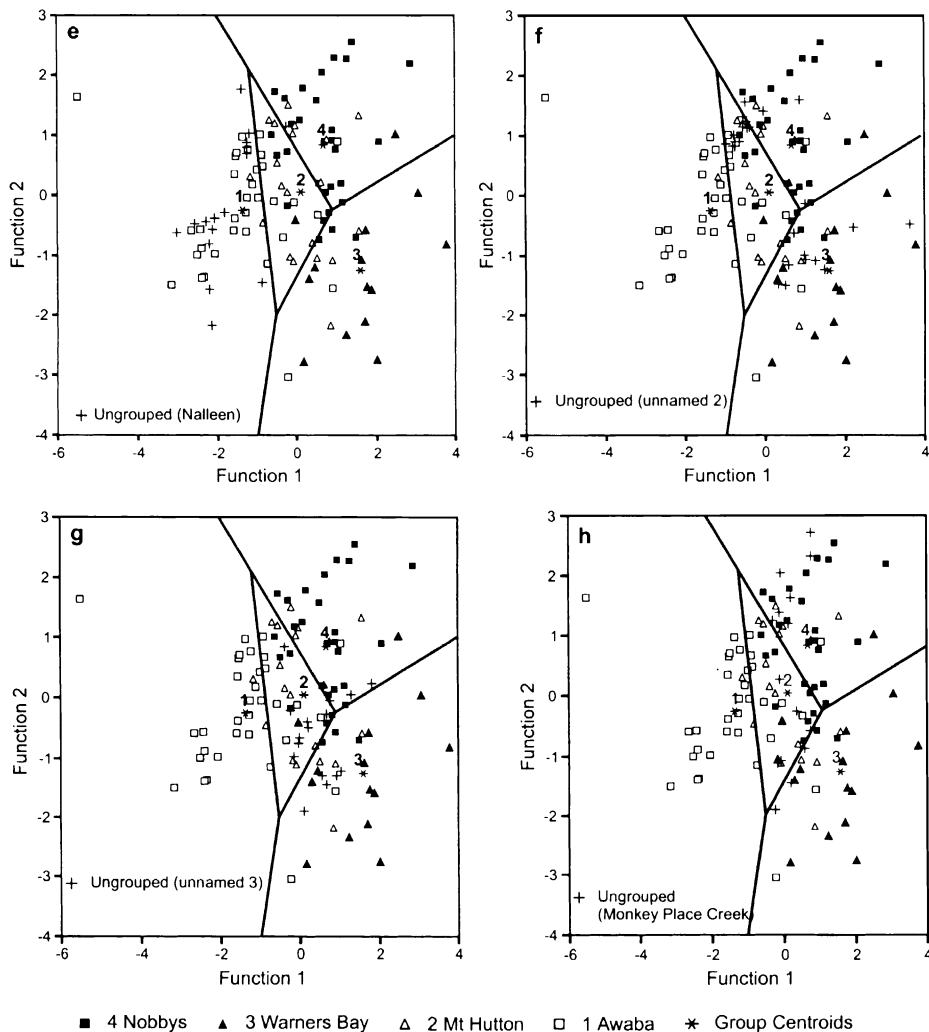


Fig. 9 (continued).

the REE patterns (Fig. 6), the enrichment of the immobile elements Hf, Th, Ta, Nb, and Zr, and depletion of Ti and P in the rock/primordial mantle patterns (Brown et al., 1984).

Two possible sources for the tuffs have been suggested, namely the SNEO and an Offshore Uplift (Harrington, 1989; Stevenson et al., 1998; Fig. 1). It is unlikely that volcanoes in the SNEO supplied the ash for the tuffs in the coal measures, as there is an absence of magmatic bodies of similar age or composition to the tuffs (Shaw and Flood, 1981, 1991). There is, however, evidence for an easterly offshore source because silicified tree trunks embedded in tuff

have been noted at Swansea Head, 20 km south of Newcastle (Diessel, 1985). According to Diessel (1985), the trees were felled by pyroclastic flows and had axes plunging towards the southwest. These observations imply that the source of the flows occurred to the northeast. Isopach maps of individual tuffs in the NCM also suggest deposition from the east, because the greatest accumulations are centred around Newcastle, thinning-out towards the west and to the north–northwest in the WCM (Hawley and Brunton, 1995; Little, 1998; Fig. 1).

Although the orientation of the axes of the silicified tree trunks provides good evidence for the gen-

eral direction of the volcanoes responsible for the flow, a more definite location could be established if volcanic rocks of the same age as the tuffs occur

elsewhere. Volcanics of similar age to the tuffs of the NCM crop out in the southern Sydney Basin and could possibly represent the source of volcanism

Table 5

Summary of predicted group membership

(i) NCM tuffs

Group	Number of cases	Predicted group membership			
		1	2	3	4
1	13	9 (69.20%)	3 (23.10%)	1 (7.70%)	0 (–)
2	7	2 (28.60%)	1 (14.30%)	4 (57.10%)	0 (–)
3	9	0 (–)	3 (33.30%)	5 (55.60%)	1 (11.10%)
4	16	0 (–)	4 (25%)	0 (–)	12 (75%)

60% of grouped cases correctly classified

(ii) NCM tonsteins

Group	Number of cases	Predicted group membership			
		1	2	3	4
1	20	18 (90%)	1 (5%)	0 (–)	1 (5%)
2	13	1 (7.70%)	2 (15.40%)	3 (23.10%)	7 (53.80%)
3	5	0 (–)	1 (20%)	4 (80%)	0 (–)
4	14	0 (–)	3 (21.40%)	1 (7.10%)	10 (71.40%)

65.38% of grouped cases correctly classified

(iii) NCM tuffs + tonsteins

Group	Number of cases	Predicted group membership			
		1	2	3	4
1	33	27 (81.8%)	1 (3%)	2 (6.1%)	3 (9.1%)
2	20	3 (15%)	8 (40%)	5 (25%)	4 (20%)
3	14	1 (7.1%)	0 (–)	12 (85.7%)	1 (7.1%)
4	30	0 (–)	8 (26.7%)	2 (6.7%)	20 (66.7%)

69.1% of grouped cases correctly classified

(iv) WCM tuffs

Group	Number of cases	Predicted group membership			
		1	2	3	4
1	16	15 (93.8%)	0 (–)	1 (6.3%)	0 (–)
2	25	0 (–)	19 (76%)	4 (16%)	2 (8%)
3	16	0 (–)	7 (43.8%)	8 (50%)	1 (6.3%)
4	15	0 (–)	2 (13.3%)	2 (13.3%)	11 (73.3%)

73.61% of grouped cases correctly classified

(v) WCM tuffs

WCM samples	Number of cases	Predicted group membership			
		Awaba	Mt. Hutton	Warners Bay	Nobbys
1	16	15 (93.8%)	0 (–)	0 (–)	1 (6.3%)
2	25	2 (8%)	6 (24%)	10 (40%)	7 (28%)
3	16	0 (–)	8 (50%)	5 (31.3%)	3 (18.8%)
4	15	0 (–)	6 (40%)	1 (6.7%)	8 (53.3%)

47.22% of grouped cases correctly classified

(Carr, 1998). However, they are basalts and basaltic andesites of shoshonitic affinity and can, therefore, be dismissed as a possible source.

Despite the fact that the shoshonites differ from the tuffs geochemically, they may provide evidence for an Offshore Uplift source in the east. Carr (1998) has noted that gabbros of similar age and composition to the shoshonites have been sampled from the Dampier Ridge. He suggested that both these rocks could have been part of a 340 km, northeast-trending belt offshore of the present coastline. A source to the east of the present coastline could account for the great thickness of the tuff in the NCM and would imply that tuffs of considerable thickness exist in offshore Permian sequences. If the volcanics are related, they represent a widespread magmatic event, which developed as a result of subduction along the east coast of Gondwanaland (Carr, 1998).

4. Discriminant statistical analysis

The major and trace element data obtained for the tuffs were subjected to multivariate statistical analysis, using the Statistical Package for the Social Sciences (SPSS, 1999) Version 10 Software Package. The stepwise method is a procedure that selects the best set of discriminating variables to form the discriminant function by forward- and backward-selection processes. At each step of the calculation, variables are removed if they do not significantly increase the discriminating power of the set. If no

variable is removed, the variable that adds to the discriminating power significantly is added to the set (Huff, 1983). Calculated with each step is the Wilks' lambda value, which is the fractional amount of within-bed variance relative to the between-bed variance that remains unaccounted for after each element is entered into the analysis (Cullen-Lollis and Huff, 1986).

In this analysis, the effects of a collection of interval level independent variables (elements) on a nominal dependent variable (classification) are calculated. In this way, it is possible to test for differences between parent groups and, if different, to assign an unknown sample to one of them. The subprogram DISCRIMINANT calculates discriminant-function coefficients and classification function coefficients, and in the stepwise mode will enter variables in the order of their explanatory power (Huff, 1983).

The effectiveness of each of the functions is represented by the corresponding eigenvalues, which measure the amount of variation within the element groups. Thus, the greater the amount of variation, or variance, the greater the separation between the tuffaceous layers. The canonical correlation for each of the functions is a measure of the effectiveness with which the coefficients computed for each element separate tuffaceous layers (Huff, 1983).

This treatment reveals the relative discriminant strength of each element, which is used to create the best set of discriminative variables and reduce the list to the minimum necessary to achieve correlation at an acceptable level of confidence. The power of

Table 6
Discriminant analysis statistics

	Function	Eigenvalue	Percentage of variance	Cumulative percentage	Canonical correlation
NCM tuffs	1	1.825	85.2	85.2	0.804
	2	0.317	14.8	100	0.491
NCM tonsteins	1	0.904	65.9	65.9	0.689
	2	0.466	34.0	99.9	0.564
	3	0.001	0.1	100	0.031
NCM tuffs + tonsteins	1	1.176	69.3	69.3	0.735
	2	0.489	28.8	98.1	0.573
	3	0.032	1.9	100	0.175
WCM tuffs	1	2.851	75.2	75.2	0.86
	2	0.929	24.5	99.6	0.694
	3	0.013	0.4	100	0.115

Table 7
Discriminant analysis statistics

Step	NCM tuffs		NCM tonsteins		NCM (comb)		WCM	
	Element	Wilks' lambda	Element	Wilks' lambda	Element	Wilks' lambda	Element	Wilks' lambda
1	Y	0.423	P ₂ O ₅	0.653	Y	0.893	TiO ₂	0.478
2	P ₂ O ₅	0.269	TiO ₂	0.472	TiO ₂	0.797	Zr	0.284
3			Ga	0.358	Ga	0.697	Th	0.175
4					Zr	0.596	P ₂ O ₅	0.133
5					P ₂ O ₅	0.516		
6					Hf	0.431		
7					Th	0.360		

discriminant analysis lies in the fact that the combination of elements, each of which have some low to moderate discriminative power, achieves discrimination superior to that of any single element (Huff, 1983).

The results of this analysis are shown in the territorial maps (Fig. 9a–h) and the statistics (eigenvalues, predicted group membership, Wilks' lambda) in Tables 5–7.

5. Geochemical correlation

5.1. NCM tuffs and tonsteins

The NCM samples were split into tuffs and tonsteins. For convenience, samples containing > 6% LOF are classified as tonsteins, the purpose of which was to test whether the altered samples could be discriminated to the same degree as the unaltered samples. Application of the discriminant analysis to the less altered tuffs shows that the Awaba Tuff and Nobbys Tuff are chemically distinct with 69.2% and 75.0% of samples falling into their predicted group (Table 5). However, the Warners Bay Tuff and in particular the Mt. Hutton Tuff, are chemically less distinct, the latter showing considerable spread on the territorial map (Fig. 9a). By contrast, the tonsteins exhibit a better separation with only the samples from the Mt. Hutton Tuff showing scatter (Fig. 9b; Table 5).

When the tuffs and tonsteins are combined, the separation improves with 81.8% of Awaba Tuff samples, 85.7% of Warners Bay Tuff samples and 66.7% of Nobbys Tuff samples falling into their predicted

groups (Table 5). However, only 40% of the samples from the Mt. Hutton Tuff are correctly classified.

5.2. WCM tuffs

Discriminant analysis reveals that the tuffs from the WCM are slightly better separated than the tuffs and tonsteins in the NCM with 73.6% correctly classified (Table 5). Of the individual tuffs, the samples from the Nalleen Tuff show the best separation with 93.8% distinct from other groups. This contrasts with the samples from the Warners Bay Tuff, which do not have a chemically unique signature, as 50% plot in the proposed group and 43.8% the Mt. Hutton Tuff region.

5.3. Correlation with the WCM

To ascertain whether tuffs in the WCM could be correlated with those in the NCM, samples of each tuff were treated as unknowns and compared against the discriminant model.

When the Nalleen Tuff was added as an ungrouped member to the NCM data set, 93.8% plot into the predicted group, indicating a clear correlation with the Awaba Tuff. Correlation of the unnamed tuff of the WCM with the Mt. Hutton Tuff (Table 1) is poor with only 24% plotting in the Mt. Hutton field, 40% plot within the Warners Bay field and 28% in the Nobbys tuff field (Fig. 9f). This wide scatter between groups indicates that this tuff does not have a unique chemical signature and therefore cannot be used for correlation. The unnamed tuff equivalent to the Warners Bay Tuff also shows a wide scatter between groups (Fig. 9g) and has a

stronger affinity with the Mt. Hutton Tuff than with the Warners Bay Tuff (Table 5).

The Nobbys Tuff and Monkey Place Creek (MPC) Tuff show a reasonable correlation; however, 40% of the ungrouped members plot in the Mt. Hutton group (Fig. 9h). It would appear that these tuffs have some chemical affinity with each other but the chemical signature is not distinctive, thus the correlation proposed by Stevenson (1999) based on lithostratigraphic grounds must be treated with caution.

5.4. Discussion

The discriminant analysis showed that a reasonable separation of the tuffs and tonsteins in the NCM, and tuffs in the WCM could be achieved on the basis of their chemical signature (Fig. 9a–d; Table 6). However, the samples of the Mt. Hutton Tuff in the NCM scatter widely on the territorial map. The discriminant analysis also revealed a poor correlation of the Warners Bay and Mt. Hutton Tuffs in the NCM with their proposed stratigraphic equivalents in the WCM (Table 1).

The reason for the chemical heterogeneity shown by some tuffs and the poor correlation between the Mt. Hutton and Warners Bay Tuffs, and the unnamed tuffs of the WCM, is unclear. Insufficient sampling cannot be the explanation for the lack of a well defined chemical signature for the Mt. Hutton Tuff because 20 analyses were carried out compared to 14 for the Warners Bay Tuff, 12 of which were correctly classified (Table 5). The chemical heterogeneity may simply be a function of the fact that samples have been taken from very thick tuffs showing several cycles of eruptive activity. In this situation, there is a greater chance of chemical inhomogeneity occurring in a tuff horizon, a problem that is rarely encountered in studies of thinly bedded bentonites (Huff et al., 1997 and references therein). With regard to the poor correlation of some tuffs between the coal measures, the possibility arises that the tuffs chosen by Stevenson (1999) are not the true correlatives of the Mt. Hutton and Warners Bay Tuffs.

Further sampling and analysis of other tuffs in the sequence adjacent to the Mt. Hutton Tuff in the NCM and to the unnamed tuffs in the WCM, are necessary. This may lead to better discrimination of

the groups within the two coal measures and to more satisfactory correlation of tuffs between them.

6. Conclusion

Studies of tuffs and tonsteins in the NCM and tuffs in the WCM indicate that most carry unique chemical fingerprints which allow them to be separated using multivariate statistical analysis. They also confirm the correlation of the Awaba Tuff of the NCM with the Nallen Tuff of the WCM and possibly the Nobbys Tuff with Monkey Place Creek Tuff proposed on lithostratigraphic grounds by Stevenson (1999; Table 1). However, the unnamed tuffs in the WCM cannot be correlated satisfactorily with the Mt. Hutton and Warners Bay Tuffs in the NCM. This suggests that the lithostratigraphic correlation suggested by Stevenson (1999) may be incorrect. The lack of unique fingerprints in some tuffs is due to their inherent chemical inhomogeneity.

The tuffs in the NCM and WCM are composed of quartz, plagioclase ($\text{An}_{54}\text{Ab}_{42}\text{Or}_4$ – $\text{An}_{33}\text{Ab}_{59}\text{Or}_8$), degraded biotite and rare K-feldspar and lithic fragments. Alteration during burial at $T < 100^\circ\text{C}$ has resulted in the formation of illite/smectite (I/S; I_{62-78}), kaolinite, siderite/ankerite and, in extreme circumstances, tonsteins dominated by I/S. The magmas responsible for the tuffs are of rhyodacitic–dacitic composition and appear to have been derived from calc-alkaline magmas erupted from volcanoes in a continental arc, offshore from the eastern margin of Gondwana.

Acknowledgements

We thank Darryl Stevenson, Carol Simpson and Paul Carr for their constructive comments on the early draft of this paper, and Warren Huff and Bruce Bohor for their incisive reviews. Steve Dick and Sharon Francis are acknowledged for their patience and skill in drafting the figures. The assistance of David Phelan with the electron microprobe analysis, and the XRF analyses of the tuffs by Jenny Zobec are very much appreciated. WK and GW acknowledge the advice given by Jennifer Wadsworth on sedimentological aspects of the project. Funding for

this project from the NSW Department of Mineral Resources and Powercoal is gratefully acknowledged.

References

- Bohor, B.F., Triplehorn, D.M., 1993. Tonsteins: altered volcanic-ash layers in coal-bearing sequences. *Geol. Soc. Am., Spec. Pap.* 285, 1–44.
- Britten, R.A., 1972. A review of the stratigraphy of the Singleton Coal Measures and its significance to coal geology and mining in the Hunter Valley region of New South Wales. *Proc. Annual Conf. Australasian Inst. Min. and Metall.*, Newcastle, pp. 11–22.
- Brown, G.C., Thorpe, R.S., Webb, P.C., 1984. The geochemical characteristics of granitoids in contrasting arcs and comments on magma sources. *J. Geol. Soc. (London)* 141, 413–426.
- Carr, P.F., 1998. Subduction related Late Permian shoshonites of the Sydney Basin, Australia. *Mineral. Petrol.* 63, 49–71.
- Collins, W.J., 1994. Escape tectonics and the redistribution of Permian basins in the southern New England Fold Belt. *Proc. 28th Newcastle Symposium on Advances in the Study of the Sydney Basin*. University of Newcastle, Newcastle, Australia, pp. 72–77.
- Crapp, C.E., Nolan, R., 1975. Newcastle district. In: Traves, D.M., King, D. (Eds.), *Economic Geology of Australia and Papua New Guinea-2: Coal*. Australian Institute of Mining and Metallurgy, Monograph 6, pp. 163–175.
- Cullen-Lollis, J., Huff, W.D., 1986. Correlation of Champlainian (Middle Ordovician) K-Bentonite beds in central Pennsylvania based on chemical fingerprinting. *J. Geol.* 94, 865–874.
- Diessel, C.F.K., 1985. Tuffs and tonsteins in the coal measures of New South Wales, Australia. *10 Int. Congr. Carbon. Strat. Geol.*, Madrid. San Martin, Madrid, 1983, vol. 4, pp. 197–211.
- Eastell, J., Willis, J.P., 1990. A low dilution fusion technique for the analysis of geological samples, method and trace element analysis. *X-ray Spectrom.* 19, 3–14.
- Ewart, A., Chappell, B.W., 1989. Trace element geochemistry. In: Johnson, R.W. (Ed.), *Intraplate Volcanism*. Cambridge Univ. Press, Australia, pp. 219–235.
- Gulson, B.L., Diessel, C.F.K., Mason, D.R., Krogh, T.E., 1990. High precision radiometric ages from the northern Sydney Basin and their implication for the Permian time interval and sedimentation rates. *Aust. J. Earth Sci.* 37, 459–469.
- Harrington, H.J., 1989. Tectonic history. In: Wolf, K.H. (Ed.), *Permian Coals of Eastern Australia: Bureau of Mineral Resources Bull.* 231, Australian Government Publication Services, Canberra, pp. 377–393.
- Hawley, S.P., Brunton, J.S., 1995. Newcastle Coalfield: Notes to accompany the 1:100 000 Newcastle Coalfield Regional Geology Map. Geological Survey Report No. GS 1995/256. Department of Mineral Resources, NSW.
- Herbert, C., 1994. Cyclic sedimentation in the lower Newcastle Coal Measures. *Proc. 28th Newcastle Symposium on Advances in the Study of the Sydney Basin*. Univ. Newcastle, Newcastle, NSW, Australia, pp. 134–141.
- Herbert, C., 1997. Relative sea level control of deposition in the Late Permian Newcastle Coal Measures of the Sydney Basin, Australia. *Sediment. Geol.* 107, 167–187.
- Hower, J., Eslinger, E.V., Hower, M.E., Perry, E.A., 1976. Mechanism of burial metamorphism of argillaceous sediment: mineralogical and chemical evidence. *Geol. Soc. Am. Bull.* 87, 725–737.
- Huff, W.D., 1983. Correlation of Middle Ordovician K-bentonites based on chemical fingerprinting. *J. Geol.* 91, 657–669.
- Huff, W.D., Kolata, D.R., 1989. Correlation of K-bentonite beds by chemical fingerprinting using multivariate statistics. In: Cross, T.A. (Ed.), *Quantitative Dynamic Stratigraphy*. Prentice-Hall, Englewood Cliffs, NJ, USA, pp. 567–577.
- Huff, W.D., Kolata, D.R., 1990. Correlation of the Ordovician Deike and Millbrig K-Bentonites between the Mississippi Valley and the Southern Appalachians. *Am. Assoc. Pet. Geol. Bull.* 74, 1736–1747.
- Huff, W.D., Bergstrom, S.M., Kolata, D.R., 1992. Gigantic Ordovician volcanic ash fall in North America and Europe: biological, tectonomagmatic, and event-stratigraphic significance. *Geology* 20, 875–878.
- Huff, W.D., Bergstrom, S.M., Kolata, D.R., Sun, H., 1997. The Lower Silurian Osmundsberg K-bentonite, Part II: mineralogy, geochemistry, chemostratigraphy and tectonomagmatic significance. *Geol. Mag.* 135, 15–26.
- Jakeš, P., Gill, J., 1970. Rare earth elements and the island arc tholeiitic series. *Earth Planet. Sci. Lett.* 9, 17–28.
- Kolata, D.R., Frost, J.K., Huff, W.D., 1986. K-Bentonites of the Ordovician Decorah Subgroup, upper Mississippi Valley: correlation by chemical fingerprinting. *Ill. Geol. Surv. Circ.* 537, 30 pp.
- Kolata, D.R., Frost, J.K., Huff, W.D., 1987. Chemical correlation of K-Bentonite beds in the Middle Ordovician Decorah Subgroup, upper Mississippi Valley. *Geology* 15, 208–211.
- Kramer, W., 1999. Stratigraphic Correlation of Tuffs in the Newcastle Coal Measures. BSc (Hons) Thesis, University of Newcastle (unpublished).
- Landenberger, B., 1996. Petrogenesis and tectono-magmatic evolution of S-type and A-type granites in the New England Batholith. PhD Thesis, University of Newcastle (unpublished).
- Little, M., 1998. Stratigraphic Analysis of the Newcastle Coal Measures, Sydney Basin Australia. BSc (PhD) Thesis, University of Newcastle (unpublished).
- Loughnan, F.C., 1962. Some tonstein-like rocks from New South Wales, Australia. *Neues Jahrb. Mineral., Abh.* 99, 29–44.
- Merriman, R.J., Peacor, D.R., 1999. Very low-grade metapelites: mineralogy, microfabrics and measuring reaction progress. In: Frey, M., Robinson, D. (Eds.), *Low Grade Metamorphism*. Blackwell, London, pp. 10–53.
- Mitchell, C.E., Goldman, D., Delano, J.W., Samson, S.D., Bergstrom, S.M., 1994. Temporal and spatial distribution of biozones and facies relative to geochemically correlated K-Bentonites in the Mid Ordovician Taconic foredeep. *Geology* 22, 715–718.
- Moore, D., Reynolds, R., 1989. X-ray Diffraction and the Identifi-

- cation and Analysis of Clay Minerals. Oxford Univ. Press, Oxford.
- Pearce, J.A., Harris, N., Tindle, A., 1984. Trace element discrimination diagrams for the tectonic interpretation of granitic rocks. *J. Petrol.* 25, 956–983.
- Rollinson, H., 1993. *Using Geochemical Data: Evaluation, Presentation, Interpretation*. Longman Group, UK.
- Shaw, S.E., Flood, R.H., 1981. The New England Batholith, Eastern Australia: geochemical variations in time and space. *J. Geophys. Res.* 86, 10530–10544.
- Shaw, S.E., Flood, R.H., 1991. A compilation of Late Permian and Triassic biotite Rb–Sr data from the New England Batholith and areas to the southeast. In: Carr, P.F. (Ed.), *Centre For Isotope Studies, Res. Report 1991–1992*. CSIRO Mineral Research Laboratory, CSIRO, Sydney, Australia, pp. 151–155.
- SPSS, 1999. SPSS 10.0. SPSS, 233S Wacker Drive, Chicago, Illinois 60606, USA.
- Stevenson, D., 1999. The Wollombi coal measures. *Proc.* 33rd Newcastle Symposium on Advances in the Study of the Sydney Basin. Univ. Newcastle, Newcastle, NSW, Australia, pp. 115–123.
- Stevenson, D., Pratt, W., Beckett, J., 1998. Stratigraphy of the hunter coalfield. In: Fityus, S., Hitchcock, P., Allman, M., Delaney, M. (Eds.), *Geotechnical Engineering and Engineering Geology in the Hunter Valley*. Proc. Aust. Geomechanics Soc., Univ. Newcastle, Newcastle, NSW, Australia, pp. 13–37.
- Sun, S.S., McDonough, W.F., 1989. Chemical and isotopic systematics of oceanic basalts: implications for mantle compositions and processes. In: Saunders, A.D., Norry, M.J. (Eds.), *Magmatism in the Ocean Basins*. Geol. Soc. Spec. Publication, vol. 42, Blackwell, Oxford, pp. 313–345.
- Winchester, J.A., Floyd, P.A., 1977. Geochemical discrimination of different magma series and their differentiation products using immobile elements. *Chem. Geol.* 20, 325–343.
- Young, G.C., Laurie, J.R., 1996. The phanerozoic timescale. In: Young, G.C., Laurie, J.R. (Eds.), *An Australian Phanerozoic Timescale*. Oxford Univ. Press, Melbourne, pp. 6–11.